TÜBİTAK

Turkish Journal of Physics

http://journals.tubitak.gov.tr/physics/

Research Article

Turk J Phys
(2013) 37: 229 – 236
© TÜBİTAK
doi:10.3906/fiz-1206-18

Effect of stepwise replacement of LiF by ZnO on structural and optical properties of $LiF.B_2O_3$ glasses

Susheel ARORA,[1,*] **Virender KUNDU,**[2] **Dev Raj GOYAL,**[1] **Anup Singh MAAN**[1]
[1]Department of Physics, Maharshi Dayanand University, Rohtak, India
[2]Department of Electronic Science, Kurukshetra University, Kurukshetra, India

Received: 29.06.2012 • **Accepted:** 11.01.2013 • **Published Online:** 19.06.2013 • **Printed:** 12.07.2013

Abstract: Zinc fluoroborate glasses with compositions *xZnO.(40 – x)LiF.60*B_2O_3*(x = 0, 5, 10, 15, and 20)* were synthesized by the melt-quench method. The amorphous nature of the glassy samples was confirmed by XRD analysis. The nature of the bonds formed and the role of various species in the composition of the glasses were examined using FTIR spectroscopy. FTIR analysis showed shifting of an absorption band with the addition of ZnO. A UV-visible study was carried out to calculate the optical band gap energy, E_g. It was found that E_g decreased with increase in concentration of ZnO up to $x = 15$ and increased slightly for $x = 20$ with the stepwise replacement of a nonoxide group (LiF) by an oxide group (ZnO). Urbach tail energy, E_U, was found to increase from $x = 0$ to $x = 15$ and then decreased slightly for $x = 20$. Theoretical optical basicity, Λ_{th}, decreased with decrease in concentration of LiF.

Key words: Fluoroborate glasses, XRD, FTIR, optical band gap energy, optical basicity

1. Introduction

Haloborate glasses have attracted the attention of researchers due to their numerous applications in the production of infrared optical components and optical fibers. In particular, $LiF.B_2O_3$ glasses are very useful in the fabrication of phosphors, solar energy converters, and a number of electronic devices [1]. The flexible variance in the structures of borate glasses with the addition of LiF has been reported [2]. We have recently reported the study of $LiF.B_2O_3$ glasses with concentrations varied by replacing LiF by Bi_2O_3 [3,4]. ZnO, being a transition metal oxide, exhibits semiconducting properties. It is used as an efficient material in ultraviolet-emitting devices [5]. When doped with fluorine and aluminum, it can be used to fabricate transparent-conducting electrodes and piezoelectric as well as ferroelectric layers [6]. ZnO, being an oxide group, when added to the glass network at the cost of LiF, which is a nonoxide group, exhibits its presence by decreasing the value of the optical band gap. Zn^{2+} ions are more polarizable than Li^+ ions and also oxygen is more polarizable than fluorine. Therefore, the replacement of LiF by ZnO may cause the overall polarizability of the glass to change, which in turn may affect the optical band gap. In the present communication, the effect of addition of ZnO on the structural and optical properties of $LiF.B_2O_3$ glasses is reported.

2. Experimental

Glass samples with compositions *xZnO.(40 – x)LiF. 60*B_2O_3*(x = 0, 5, 10, 15, and 20)* were synthesized through the traditional melt-quench method using ZnO, LiF, and H_3BO_3 reagent grade powders. Various powdered

*Correspondence: susheel_arora@yahoo.com

materials were taken in grams equal to their molecular masses and then mixed uniformly according to their percentage presence in various samples. The mixture was heated at 1273 K for 30 min to get a bubble-free melt. The melt so formed was pressed between 2 carbon plates at room temperature. Thin pallets of the glassy samples with an average thickness of 1 mm were obtained.

The amorphous nature of the samples was tested on a Regaku X-ray diffractometer using Cu-Kα radiations. Samples were ground properly to powdered form, which in turn was placed in the diffractometer and rotated at the rate of 1°/min. A plot of diffracted intensity and the angle was obtained.

FTIR spectroscopy on the thin pallets of the samples was carried out in the range of 652 cm^{-1} to 4000 cm^{-1} at room temperature using a PerkinElmer FTIR spectrophotometer. Plots between % transmission and wave number were obtained.

The absorption of UV-Visible radiations in the reported samples was studied using a PerkinElmer UV-Visible spectrophotometer. Plots between absorption and wavelength of incident radiations were obtained.

3. Results and discussion

3.1. XRD analysis

The X-ray diffraction patterns for the samples *xZnO.(40 – x)LiF.60*B_2O_3*(x = 0, 5, 10, 15, and 20)* are plotted in Figure 1. There are no peaks in any of the plots, characterizing the samples as amorphous in nature.

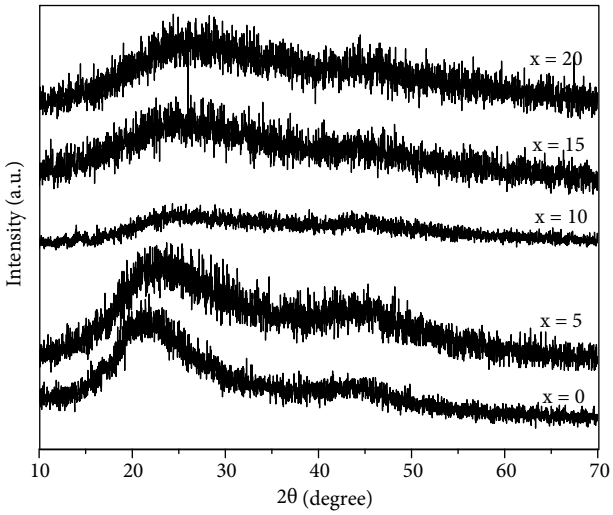

Figure 1. XRD plots for samples with *x = 0, 5, 10, 15, and 20* in the compositions *xZnO.(40 – x)LiF.60* B_2O_3.

3.2. FTIR analysis

FTIR spectra for the series of glassy samples with compositions *xZnO.(40 – x)LiF.60*B_2O_3*(x = 0, 5, 10, 15, and 20)* are shown in Figure 2. Absorption was recorded in the range 652 cm^{-1} to 4000 cm^{-1}. However, the results are reported in the range of 652 cm^{-1} to 1650 cm^{-1}, as all the absorptions observed in the higher range were due to water groups.

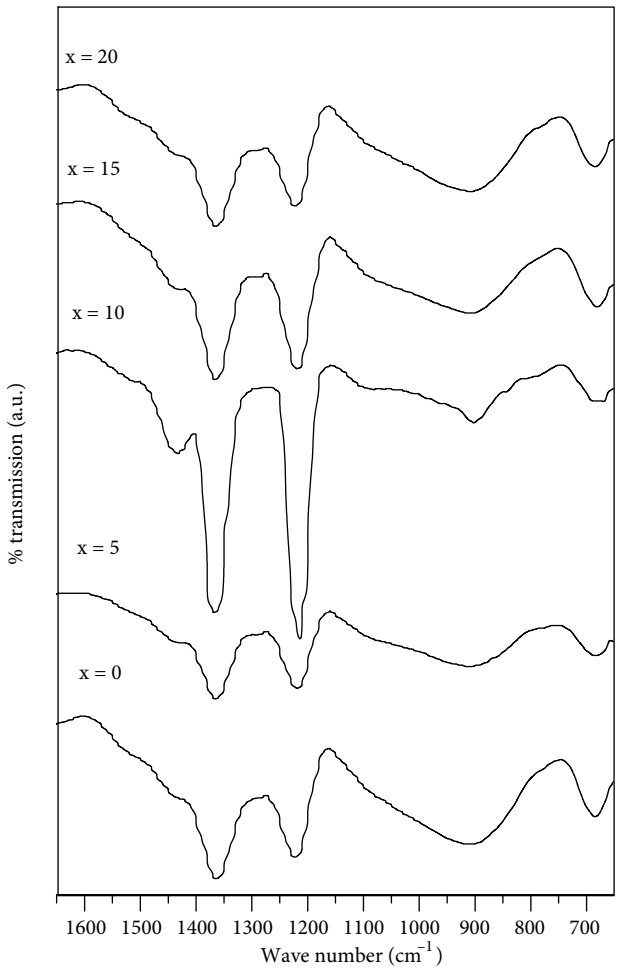

Figure 2. FTIR plots for samples with $x = 0, 5, 10, 15, and\ 20$ in the compositions $xZnO.(40 - x)LiF.60\ B_2O_3$.

There was an absorption band appearing at around 685 cm^{-1} in all the compositions. This is attributed to the bending of B-O-B linkage in the borate network [7]. There appears an absorption band at around 910 cm^{-1} for each of the reported compositions, which is due to the B-O bond stretching in BO_4 units of di-borate groups [8]. An absorption band around 1098 cm^{-1}, which is almost absent in the composition with $x = 0$, shows its small but significant presence in the compositions with concentrations of ZnO. This band is a signature of the absorption made by penta-borate and di-borate groups [9,10]. These groups increase with the increase in ZnO concentration as it joins the glass network with the replacement of some concentration of LiF. Therefore, a nonoxide group gets replaced by an oxide group, increasing the possibilities of penta-borate and di-borate groups being generated.

The absorption range 1160–1600 cm^{-1}, as reported [8,9,11], is due to the B-O bond stretching vibrations in BO_3 units. In this particular absorption range, 2 bands are originating. The first band is centered at 1220 cm^{-1}. This absorption is due to symmetric stretching vibrations of B–O bonds in BO_3 units from meta- and ortho-borate groups [8–12]. The second band is centered at 1365 cm^{-1} for the composition with $x = 0$ and at 1370 cm^{-1} for other compositions. This absorption is assigned to the asymmetric stretching vibrations in BO_3 and BO_3^- units [8,9,12]. The shift of this band towards higher wave number with ZnO content may be due to

the formation of bridging bond Zn-O-B [13]. Another absorption band is observed at 1438 cm^{-1}, which is due to BO stretching of BO_3 units in varied types of borate groups [8]. All absorptions are listed in Table 1.

Table 1. FTIR absorption assignments of the samples with *x = 0, 5, 10, 15, and 20* in the compositions *xZnO.(40 – x)LiF.60* B_2O_3.

Wave number (cm^{-1})	Assignment
685	Bending of B-O-B linkage in borate network
910	B-O bond stretching in BO_4 units
1098	Pentaborate and diborate species
1220	Stretching vibrations of B-O bonds in BO_3 units from meta and ortho-borate
1365, 1370	B-O asymmetric stretching vibrations in BO_3 and BO_3^- units and Zn-O-B units
1438	B-O stretching vibrations of BO_3 units from varied types of borate groups

3.3. Optical analysis

A series of samples in the compositions *xZnO.(40 – x)LiF.60*B_2O_3*(x = 0, 5, 10, 15, and 20)* were tested for absorption of ultraviolet and visible radiations at room temperature. Figure 3 depicts the absorption profile of all the glassy samples. These plots show the variations in absorption coefficient $\alpha(\nu)$ against wavelength. The absorption coefficient $\alpha(\nu)$ is related to the incident intensity (I_i), transmitted intensity (I_t), and thickness of the sample (t) [14] as

$$\alpha(\nu) = (1/t)ln(I_i/I_t).$$

The absence of a sharp absorption edge in all the plots confirms the amorphous nature of the samples, which is in agreement with the results of XRD and FTIR.

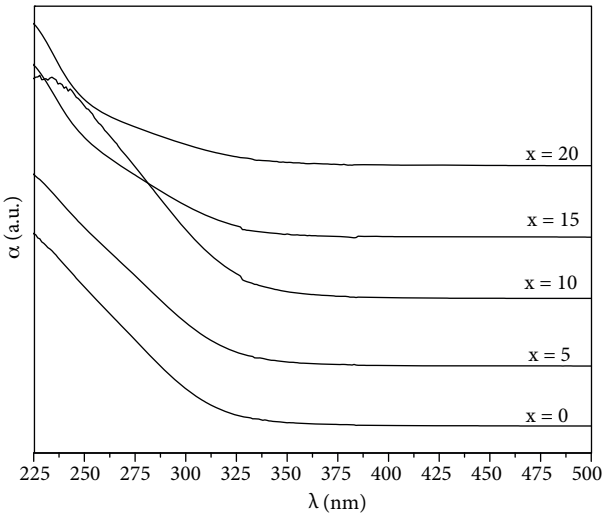

Figure 3. Optical absorption coefficient verses wavelength plots for samples with *x = 0, 5, 10, 15, and 20* in the compositions *xZnO.(40 – x)LiF.60* B_2O_3.

Optical band gap is an important parameter to characterize a material in terms of its transparency for a range of electromagnetic radiations. Optical band gap (E_g) is calculated in terms of the absorption coefficient $\alpha(\nu)$ [14] as

$$\alpha h\nu = B(h\nu - E_g)^r.$$

Here ν is the frequency of the incident radiations and B is a constant called band tailing parameter. The value of index r depends on the nature of the transitions taking place in the samples. For indirect allowed and forbidden transitions, r = 2 and 3, respectively, and for direct allowed and forbidden transitions it is 1/2 and 2/3, respectively.

Furthermore, NBOs have larger magnitude of negative charge as compared to that on bridging oxygens. This is why the materials with larger numbers of NBOs are more polarizable and vice versa. This is also the reason for the decrease in the optical band gap with increase in the number of NBOs.

Figures 4 and 5 depict Tauc's plots [$(\alpha\ h\nu)^{1/r}$ verses $h\nu$, r = 2, 3] for various samples. Extrapolating the linear region of Tauc's plots, one gets the intercepts along the $h\nu$-axis, which are the values of optical band gap energies for various samples. Values of E_g and B are listed in Table 2 and the variations in E_g with composition are plotted in Figure 6. There is a continuous decrease in the value of optical band gap energy from $x = 0$ to $x = 15$, which increases slightly for $x = 20$. Increase in ZnO concentration encourages the formation of BO_4 units, which further are being converted in BO_3^- units with one nonbridging oxygen atom. This is the reason behind the decrease in the optical band gap of the material. In the sample with $x = 20$ a slight increase in the optical band gap energy may be due to a small concentration of LiF, which allows ZnO to be connected in the glass network in a manner to decrease the number of NBOs. In the low absorption region of Tauc's plot, the absorption coefficient is related to photon energy [15] as

$$\alpha \sim \exp(h\nu/E_U).$$

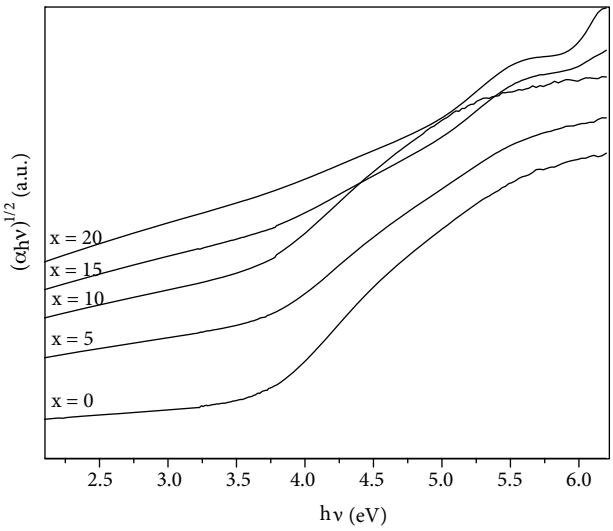

Figure 4. Tauc's plots with r = 2 for samples with $x = 0$, *5, 10, 15, and 20* in the compositions *xZnO.(40 – x)LiF.60* B_2O_3.

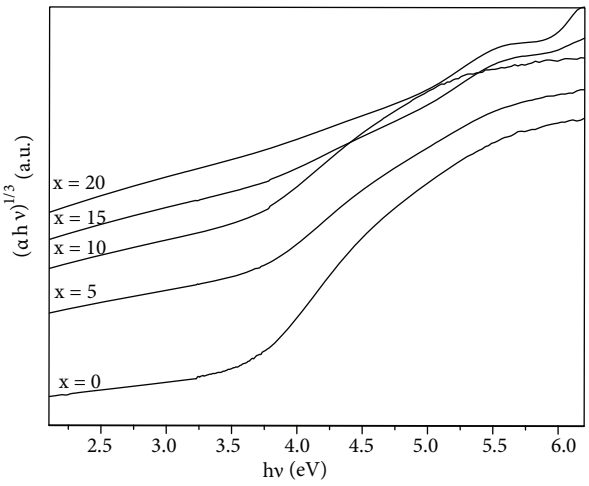

Figure 5. Tauc's plots with r = 3 for samples with $x = 0$, *5, 10, 15, and 20* in the compositions *xZnO.(40 – x)LiF.60* B_2O_3.

Here E_U is called Urbach tail energy, which corresponds to the width of tail states in the mobility gap. Tail states arise due to the disorder present in the glass structure, causing the mobility edges to enter the mobility gap. Formation of such localized states can thus be attributed to the random potential functions [16].

Electronic transitions involved in these states are generally phonon assisted transitions [17,18]. Formation of such states makes the material an indirect band gap material.

Table 2. Cutoff wavelength (λ_{cutoff}), optical band gap energy (E_g), Urbach energy (E_U), and theoretical optical basicity (Λ_{th}) for the samples with $x = 0, 5, 10, 15,$ *and 20* in the compositions $xZnO.(40 - x)LiF.60\ B_2O_3$.

x (mol%)	λ_{cutoff} (nm)	r = 2		r = 3		E_U (eV)	Λ_{th}
		E_g (eV)	B $(\text{cm eV})^{-1}$	E_g (eV)	B $(\text{cm eV})^{-1}$		
0	334	3.32	6.79	3.14	17.68	0.510	0.5266
5	369	2.56	0.87	2.39	1.37	1.000	0.5128
10	393	2.17	1.00	1.82	1.52	1.280	0.4998
15	342	2.00	0.33	1.24	0.24	2.246	0.4875
20	386	2.12	0.20	1.36	0.12	2.145	0.4758

E_U is calculated for all the reported samples from the inverses of the slopes of the linear parts of the Urbach plots (ln α v/s hν), as shown in Figure 7. Values of E_U are listed in Table 2 and variation in E_U is plotted against the composition in Figure 8. There is an increase in the value of E_U with ZnO concentration from $x = 0$ to $x = 15$ and a slight decrease for $x = 20$. This is again attributed to the structural changes taking place with the increasing concentrations of ZnO.

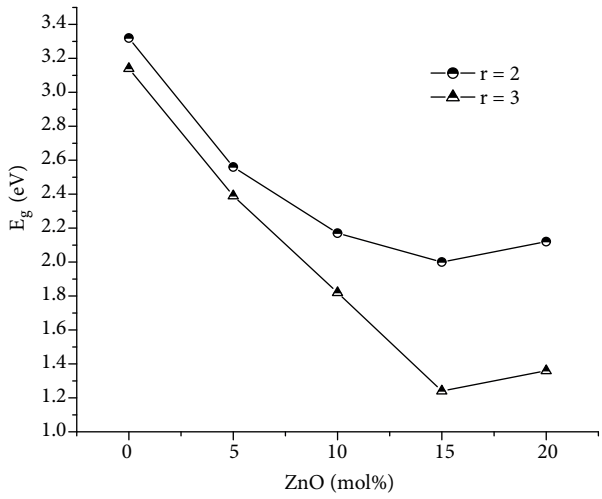

Figure 6. Variation of Eg with composition for samples with $x = 0, 5, 10, 15,$ *and 20* in the compositions $xZnO.(40 - x)LiF.60\ B_2O_3$.

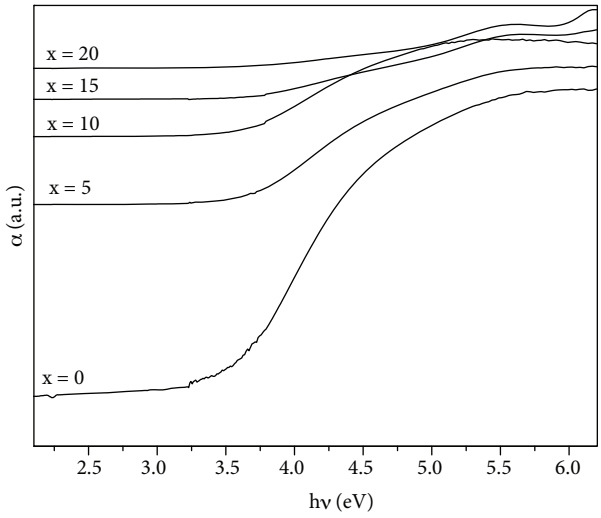

Figure 7. Urbach plots for samples with $x = 0, 5, 10, 15,$ *and 20* in the compositions $xZnO.(40 - x)LiF.60\ B_2O_3$.

Optical basicity is another parameter related to the optical properties of the glasses. Electronic polarizability and optical basicity have an intrinsic relationship. Optical basicity is expressed in terms of the electron density carried by anions. Theoretical optical basicity for the present series of samples is calculated using the following formula [19]:

$$\Lambda_{th} = \Sigma(Z_i r_i)/(Z'_o \gamma_i).$$

Here r_i is the ratio of number of cations 'i' to total number of oxide ions, γ_i is basicity modulating factor, Z_i is the oxidation number of cations 'i', and Z'_o is the oxidation number of oxide anions. Values of Λ_{th} are

listed in Table 2. It is observed that the stepwise replacement of LiF by ZnO decreases the theoretical optical basicity of the samples.

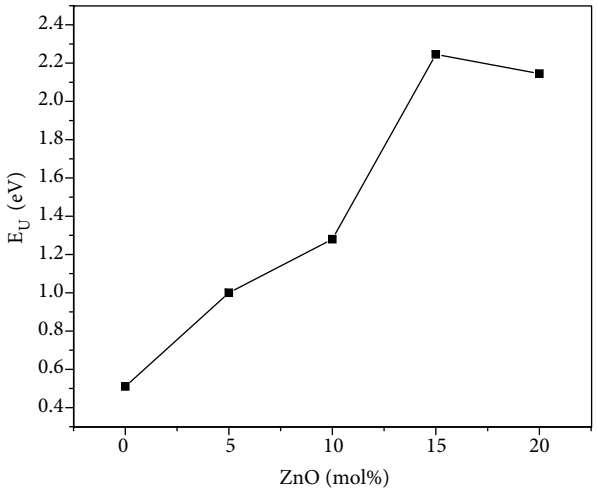

Figure 8. Variation in Urbach tail energy with composition for samples with $x = 0, 5, 10, 15, and\ 20$ in the compositions $xZnO.(40 - x)LiF.60\ B_2O_3$.

4. Conclusions

The following conclusions can be drawn from the study of samples with compositions $xZnO.(40 - x)LiF.60B_2O_3 (x = 0, 5, 10, 15, and\ 20)$:

1. From XRD analysis it can be concluded that the samples are of amorphous nature as there is no peak in the pattern.

2. FTIR spectroscopy shows shifting of a band centered at 1365 cm^{-1} to 1370 cm^{-1}, which is an indicator of structural modifications in the glass network.

3. Optical absorption study reveals that the samples are indirect band gap materials. Stepwise replacement of a less polarizable material (LiF) with a more polarizable material (ZnO) results in a decrease in the optical band gap energy from $x = 0$ to $x = 15$. It increases slightly for $x = 20$, which might be due to a greatly reduced concentration of LiF, allowing ZnO to be so connected in the glass network that the number of NBOs decreases again. Theoretical optical basicity decreases with decrease in concentration of LiF.

Acknowledgment

The financial support provided to one of the authors (Susheel Arora) by CSIR, New Delhi (India), is gratefully acknowledged.

References

[1] V. R. Kumar, B. Apparao and N. Veeraiah, *Bull. Mater. Sci.*, **21**, (1998), 341.

[2] I. Z. Hager, *J. Phys. Chem. Solids,* **70**, (2009), 210.

[3] S. Arora, V. Kundu, D. R. Goyal, and A. S. Maan, *ISRN Spectroscopy*, **2012**, (2012), 896492(1-5).

[4] S. Arora, V. Kundu, D. R. Goyal, and A. S. Maan, *ISRN Optics*, **2012**, (2012), 193185(1-7).

[5] A. Sasaki, W. Hara, A. Matsuda, N. Tateda, S. Otaka, S. Akiba, K. Saito, T. Yodo, M. Yoshimoto, *Appl. Phys. Lett,*. **86**, (2005), 231911.

[6] S. Fujihara, C. Sasaki and T. Kimura, *Key Eng. Mater.,* **181**, (2000), 109.

[7] L. Baja, R. Stefan, W. Kiefer and S. Simon, *J. Raman Spectrosc.*, **36**, (2005), 262.

[8] P. Paşcuţă, M. Boşca, S. Rada, M. Culea, I. Bratu and E. Culea, *J. Optoelectron. Adv. M.*, **10**, (2008), 2416.

[9] V. Kundu, R. L. Dhiman, D. R. Goyal and A. S. Maan, *J. Optoelectron. Adv. M.*, **10**, (2008), 2765.

[10] E. I. Kamitsos, M. A. Karakassides and G. D. Chryssikos, *J. Phys. Chem.*, **91**, (1987), 1073.

[11] C. Feifei, D. Shixun, N. Qiuhua, X. Tiefeng, S. Xiang and W. Xunsi, *J. Wuhan University of Tech.-Mater. Sci.,* **24**, (2009), 716.

[12] I. Ardelean and S. Cora, *J Mater Sci. - Mater Electron*, **19**, (2008), 584.

[13] J. N. Ayuni, M. K. Halimah, Z. A. Talib, H. A. A. Sidek, W. M. Daud, A. W. Zaidan and A. M. Khamirul, *IOP Conference Series: Materials Science and Engineering*, **17**, (2001), 012027.

[14] E. A. Devis and N. F. Mott, *Phil. Magn.*, **22**, (1970), 903.

[15] F. Urbach, *Phys. Rev.*, **92**, (1953), 1324.

[16] A. A. Kutub, A. E. Mohamed-Osman, and C. A. Hogarth, *J. Mater. Sci.* **21**, (1986), 3517.

[17] C. Dayanand, G. Bhikshamaiah, and M. Salagram, *Mater. Lett.*, **23**, (1995), 309.

[18] K. L. Chopra and S. K. Bahl, *Thin Solid Films*, **11**, (1972), 377.

[19] J. A. Duffy and M. D. Ingram, *J. Inorg. Nucl. Chem.*, **37**, (1975), 1203.